Supplement of Biogeosciences, 15, 1047–1064, 2018
https://doi.org/10.5194/bg-15-1047-2018-supplement

Biogeosciences Open Access EGU

Supplement of

Preliminary evaluation of the potential of tree-ring cellulose content as a novel supplementary proxy in dendroclimatology

Malin M. Ziehmer et al.

Correspondence to: Malin M. Ziehmer (ziehmer@climate.unibe.ch)

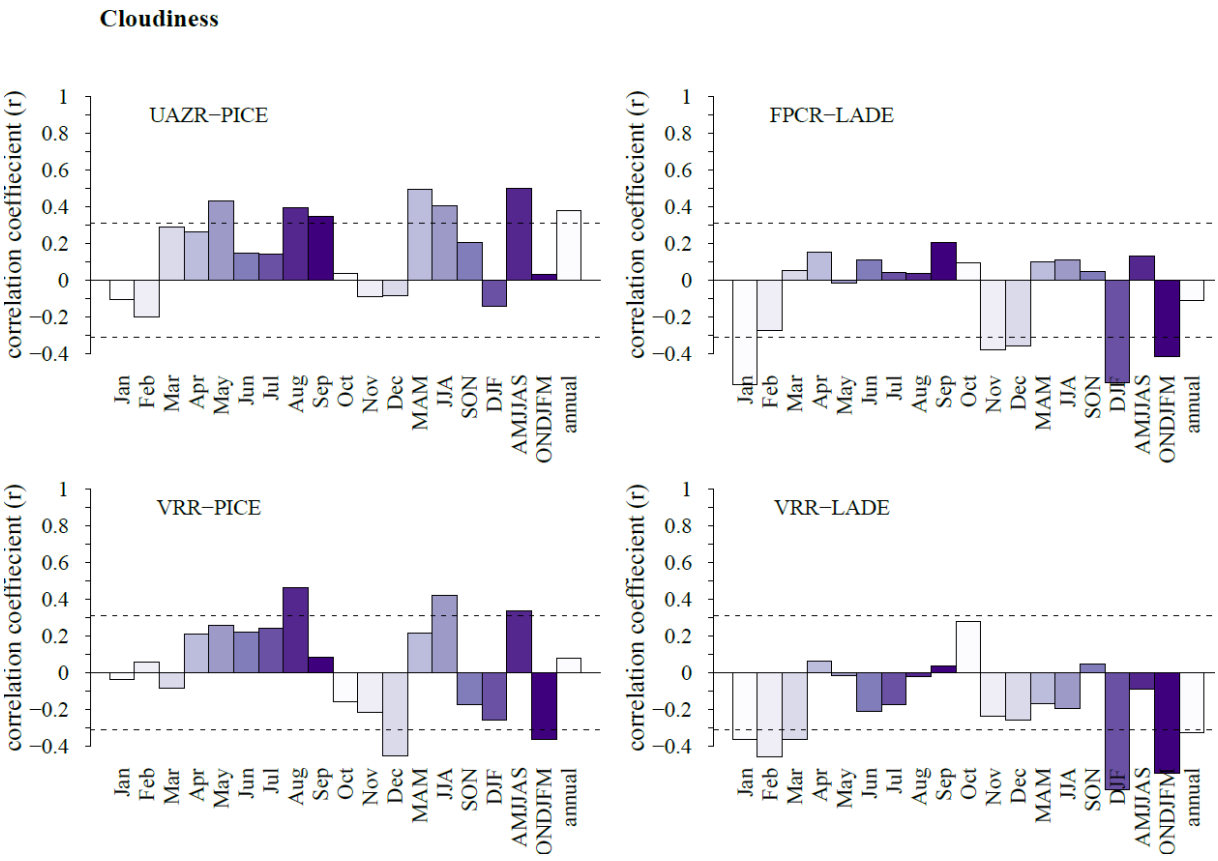

Fig. S1. Pearson's correlation coefficient for mean CC (%) and cloudiness anomalies (with reference to 1961–1990) for the period 1865–2005 AD. UAZR and FPCR are correlated with HISTALP NW region data, whereas VRR species are correlated with the SW region dataset. The dashed horizontal lines indicate the level of significance ($p<0.05$).

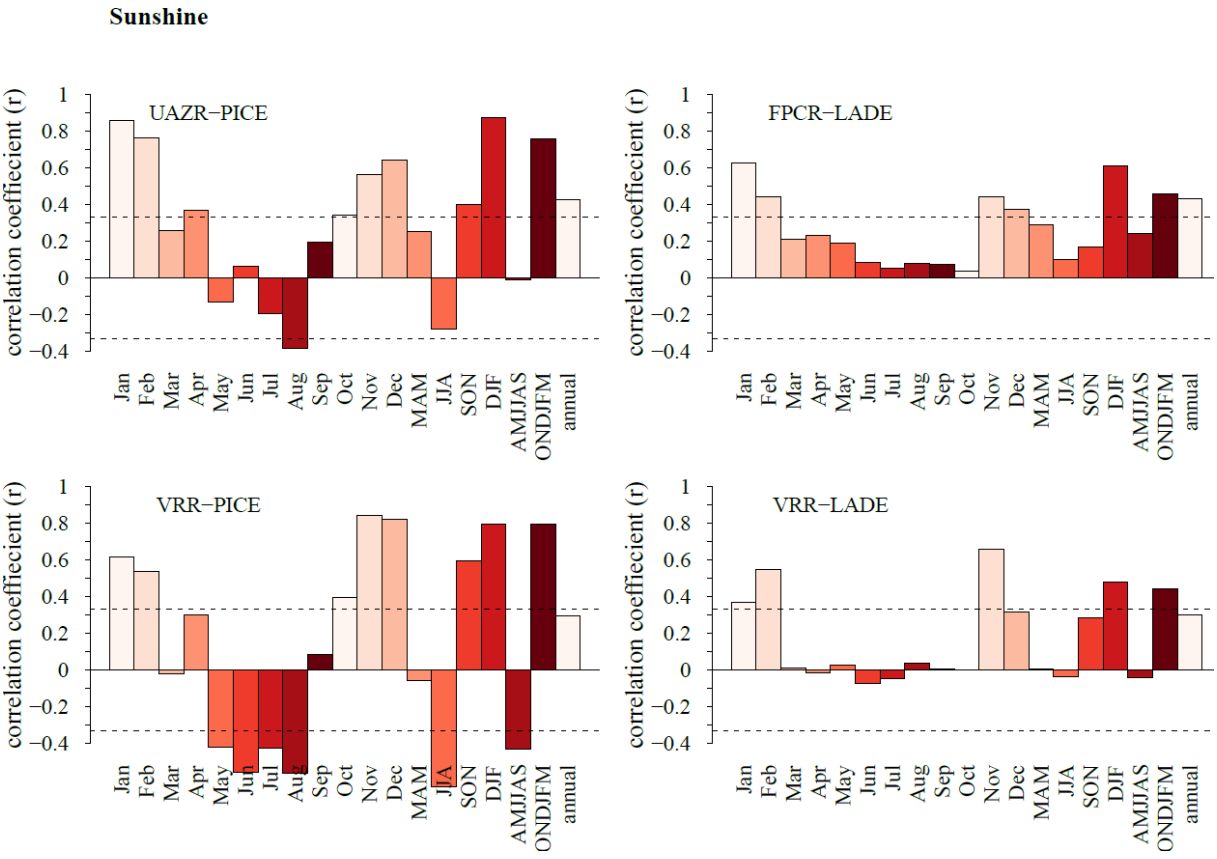

Fig. S2. Pearson's correlation coefficient for mean CC (%) and sunshine anomalies (with reference to 1961–1990) for the period 1865–2005 AD. UAZR and FPCR are correlated with HISTALP NW region data, whereas VRR species are correlated with the SW region dataset. The dashed horizontal lines indicate the level of significance ($p<0.05$).

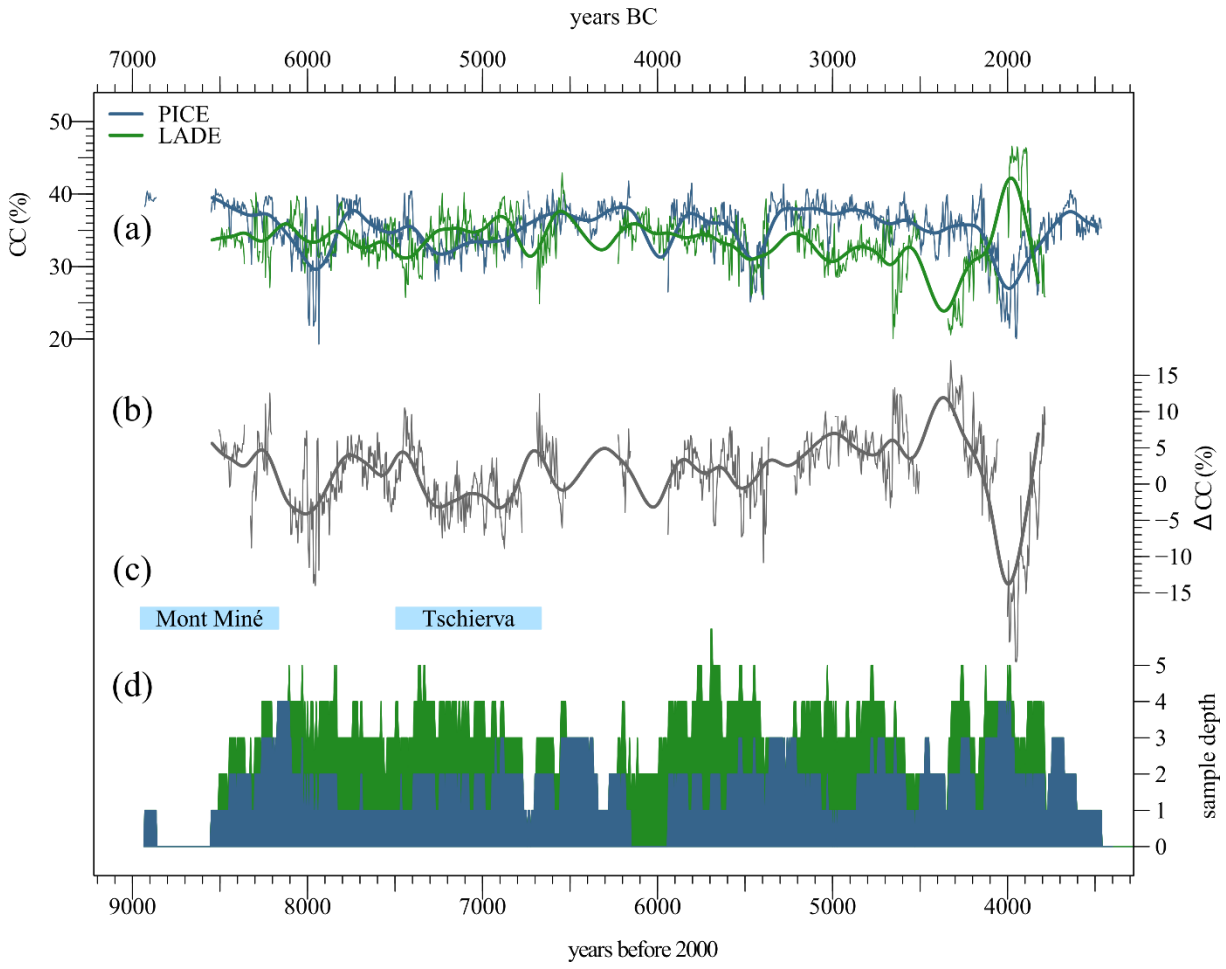

Fig. S3. Tree-species related CC (%) variability during the Holocene. Shown are (a) the mean CC (%) series for LADE (green) and PICE (blue) with corresponding smoothing lines indicating their low-frequency trends, (b) the mean difference between the species given as delta CC (%) (dark grey) and (d) the sample replication (bottom) indicating the number of samples contributing to the mean CC (%) series per species. Blue rectangles (c) mark phases where wood samples stem almost exclusively from a single glacier site.

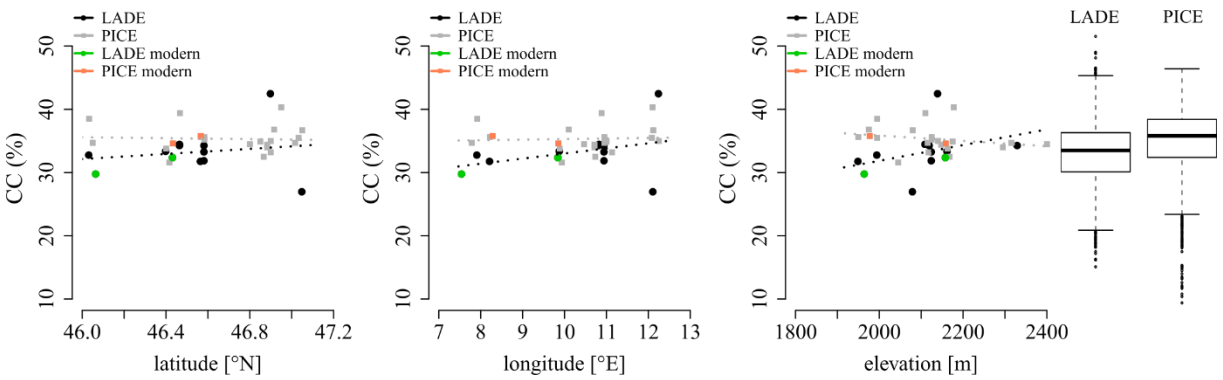

Fig. S4. Effects of site gradients in latitude (left), longitude (centre) and elevation (right) on the mean CC (%) of both individual modern (coloured) and Holocene wood samples. Mean CC (%) is calculated as the arithmetic mean of tree average values per site. Shown linear regressions per species are non-significant (p>0.05). Boxplots (right) indicate the distribution of CC (%) values for the two tree species over all sites and samples.

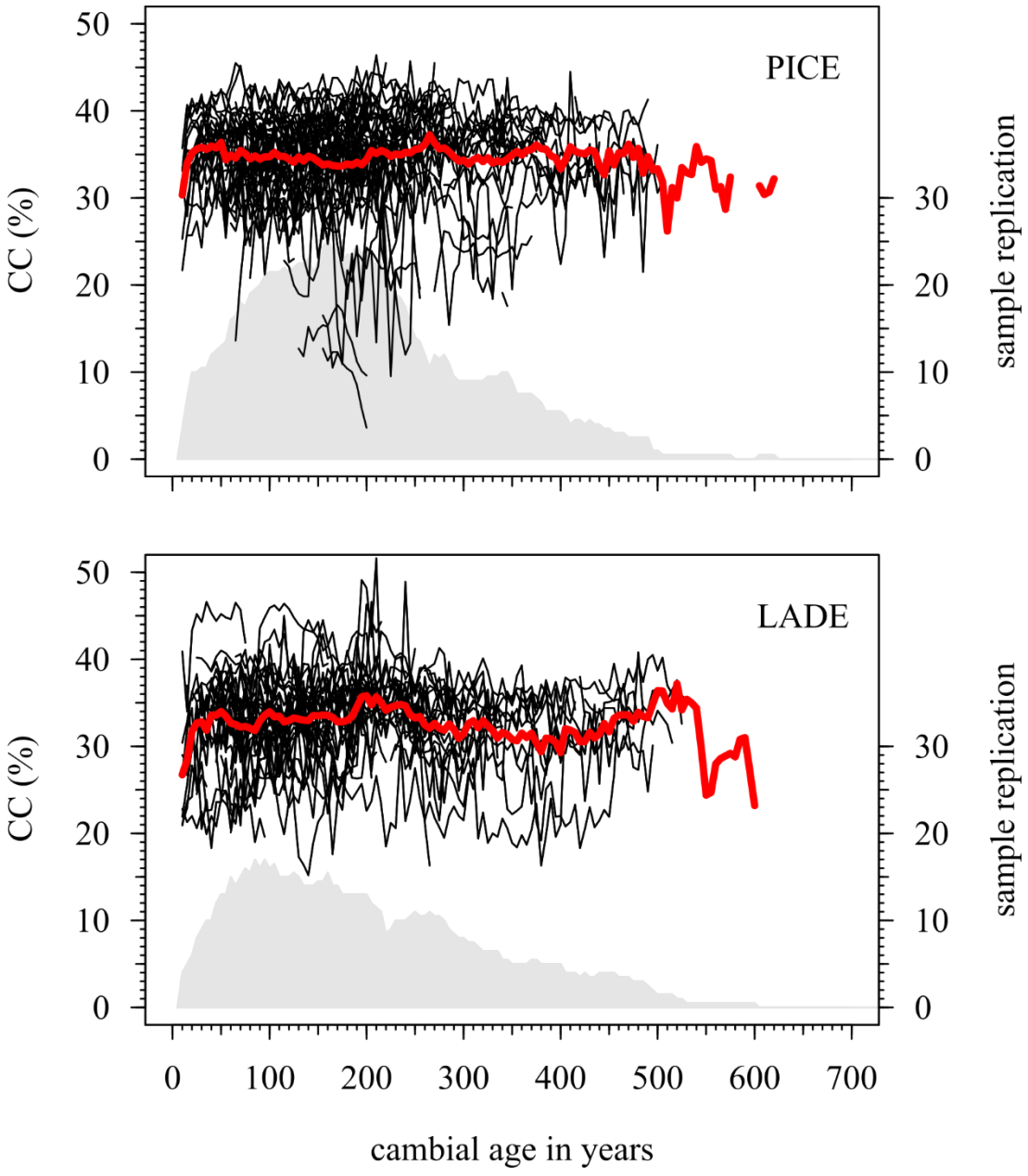

Fig. S5. CC (%) in *Pinus cembra* L. (PICE) and *Larix decidua* Mill. (LADE) aligned according to their cambial age in years (pith offset estimation is considered here). Shown are the individual series in black and the mean in red, as well as the sample replication indicated by the grey area at the bottom of each graph.

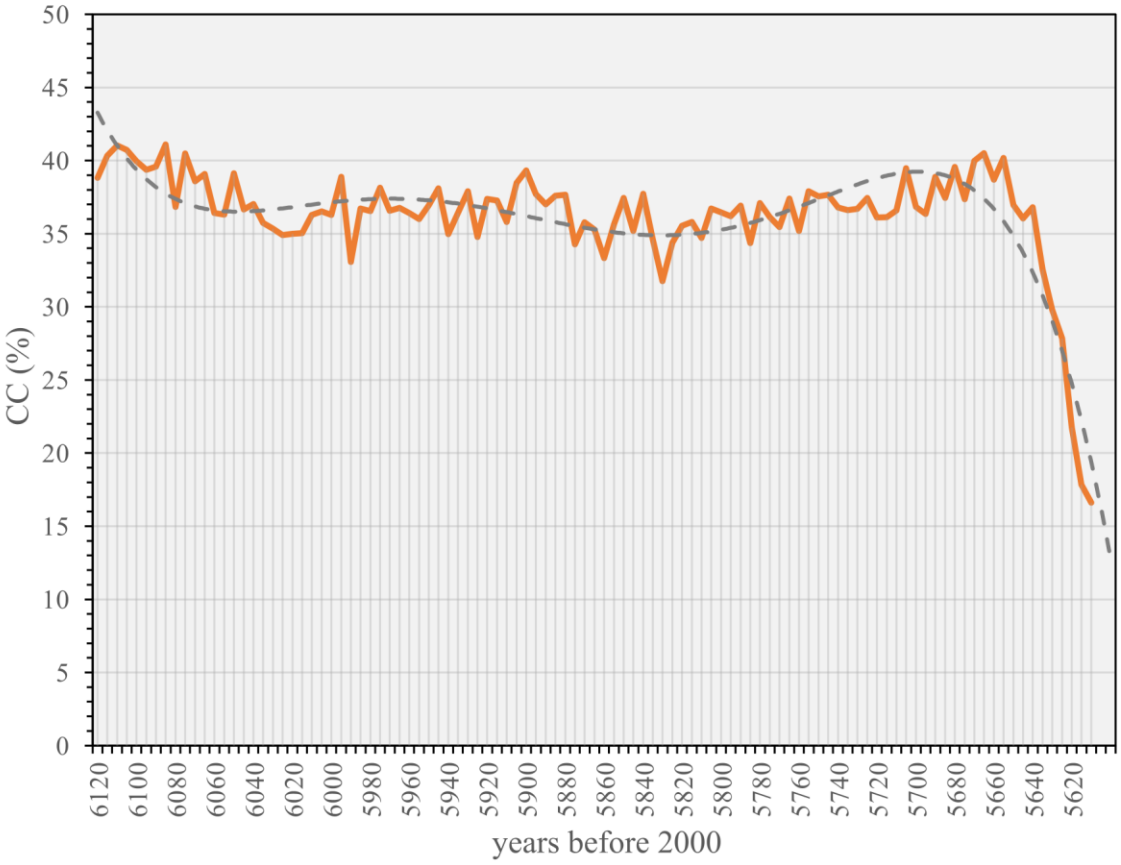

Fig. S6. Example of CC (%) variations and degradation in a *Larix decidua* Mill. tree (ULFI-47). The tree exhibits a long-term trend in its CC (%) series, followed by a rapid decrease of CC (%) in its outermost rings, which is attributed to degradation of CC (%) due to exposition to weathering. Still, most of the tree is well preserved and suitable for CC (%) analysis.

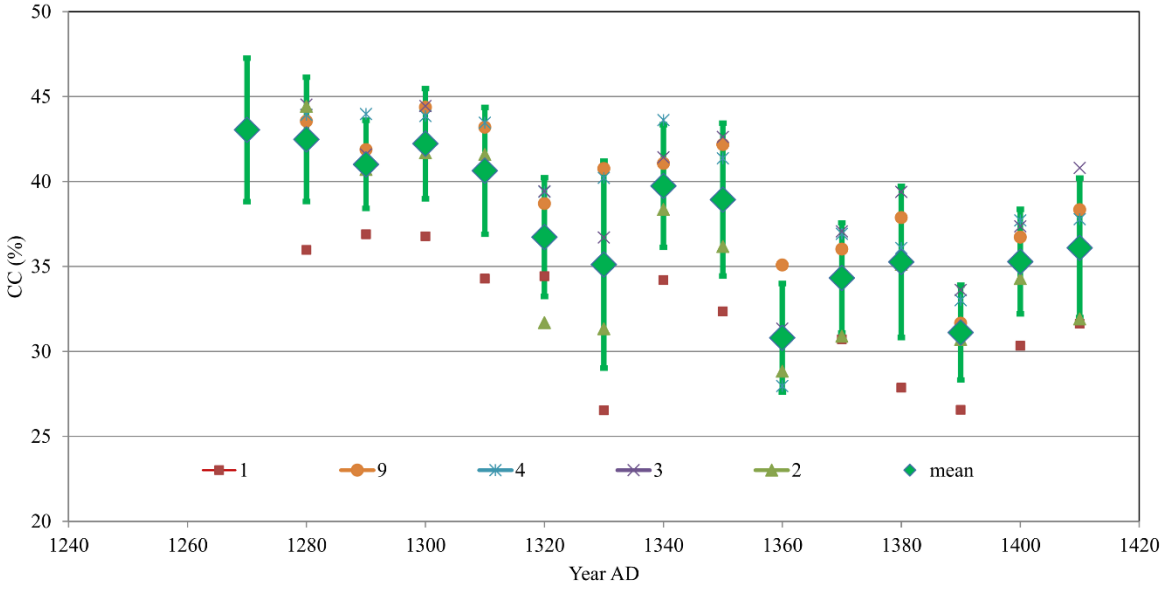

Fig. S7. Variability of CC (%) in larch tree rings from Lötschental (CH). The numbers correspond to tree cores from different trees.

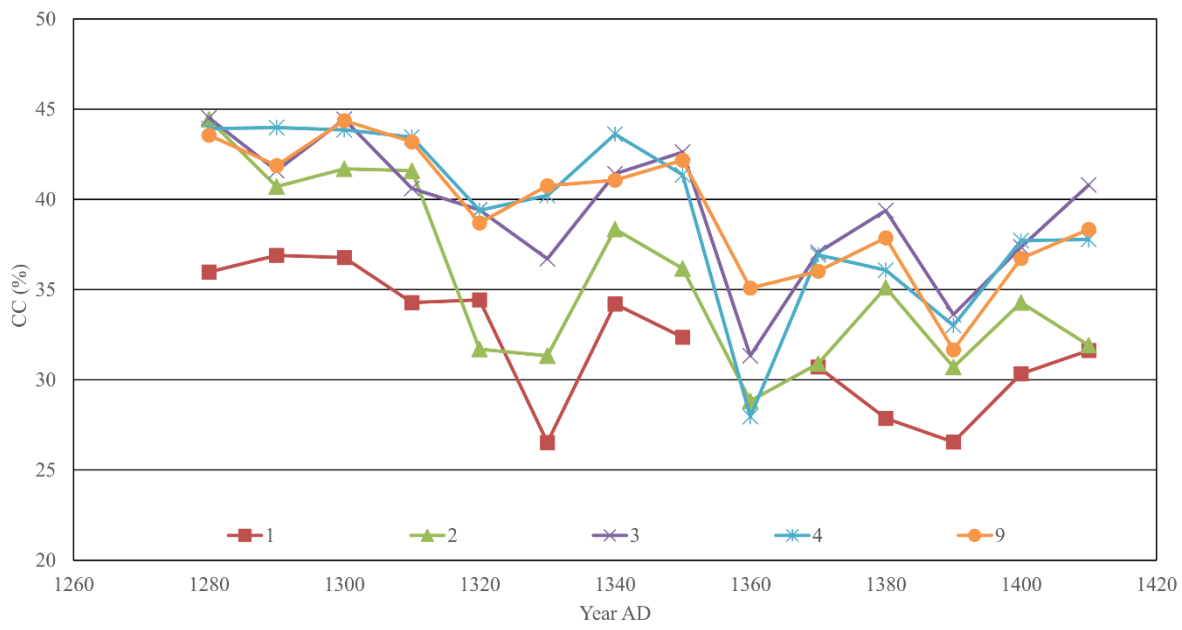

Fig. S8. Temporal variability of CC (%) in larch tree ring series from Lötschental (CH). The numbers correspond to tree cores from different trees.